

Dinuclear Mn(II), Ni(II), and Zn(II) Complexes Bridged by Bis(*p*-nitrophenyl) Phosphate Ion: Relevance to Bimetallic Phosphodiesterase

Hitomi Shiraishi, Reiko Jikido, Kanako Matsufuji, Tatsuaki Nakanishi, Takuya Shiga, Masaaki Ohba,† Ken Sakai, Hiroshi Kitagawa, and Hisashi Ōkawa*

Department of Chemistry, Faculty of Science, Kyushu University, Hakozaki 6-10-1, Higashi-ku, Fukuoka 812-8581

Received December 24, 2004; E-mail: okawascc@mbox.nc.kyushu-u.ac.jp

2,6-Bis[*N*,*N*-di(2-pyridylmethyl)aminomethyl]-4-methylphenol (Hbpmp) has afforded dinuclear Mn(II), Ni(II), and Zn(II) complexes with two bis(*p*-nitrophenyl) phosphate (BNP^-) ions, $[M_2(bpmp)(bnp)_2]ClO_4$ (M = Mn (**1**), Ni (**2**), Zn (**3**)). The structure of **1**·2MeCN has been determined by the single crystal X-ray method. It has a dinuclear core structure bridged by the phenolic oxygen atom of $bpmp^-$ and two BNP^- ions. Each metal center has a pseudo octahedral geometry with an average Mn-to-donor bond distance of 2.207 Å. Physicochemical properties of **1**–**3** are studied and their relevance to biological phosphodiesterase is discussed.

Bimetallic cores exist at active sites of many metalloenzymes and play an essential role in biological systems.[1] Dinuclear or trinuclear Zn cores are found at the active sites of phosphoesterases.[2–5] It is known that phosphotriesterases[2] use a pair of Zn ions to facilitate the concerted binding of a substrate at one Zn center and the nucleophilic attack of hydroxide or activated water provided at the adjacent Zn center. Phosphodiesterases such as phospholipase C[3] and P1 nuclease[4] require an additional Zn ion to hydrolyze phosphodiester. It is considered that the phosphodiesterases utilize a trinuclear Zn core to bind a bidentate phosphodiester on a dinuclear Zn unit and provide the nucleophile (hydroxide or activated water) on the third Zn center. Another class of phosphodiesterases has a dinuclear FeFe,[6] FeZn,[7,8] FeMn,[9] or MnMn[10] core instead of trinuclear Zn core. Thus, model studies of the bimetallic phosphodiesterases using homo- and heterodinuclear metal complexes are becoming a current subject.[11–18]

In order to gain an insight into the hydrolytic function of bimetallic phosphodiesterases, phosphodiester adducts of dinuclear metal complexes are informative.[17,19–22] In this work, phosphodiester adducts of dinuclear Mn(II), Ni(II), and Zn(II) complexes, $[M_2(bpmp)(bnp)_2]ClO_4$ (M = Mn (**1**), Ni (**2**), and Cu (**3**)), have been prepared, where Hbpmp is 2,6-bis[*N*,*N*-di(2-pyridylmethyl)aminomethyl]-4-methylphenol (Fig. 1) and BNP^- is bis(*p*-nitrophenyl) phosphate ion. The structure of **1**·2MeCN is determined to demonstrate a bis(μ-bnp)-μ-phenolato dinuclear structure. Physicochemical properties of **1**–**3** are examined and their relevance to biological phosphodiesterase is discussed.

Experimental

Physical Measurements. Elemental analyses of carbon, hydrogen and nitrogen were obtained at The Service Center of Elemental Analysis of Kyushu University. Metal analyses were obtained using a Shimadzu AA-680 Atomic Absorption/Flame Emission Spectrophotometer. Infrared spectra were measured using a KBr disk on a PERKIN ELMER Spectrum BX FT-IR system. Electronic absorption spectra in dimethyl sulfoxide (DMSO) were recorded on a Shimadzu UV-3100PC spectrophotometer. Magnetic susceptibilities of powdered samples were measured on a Quantum Design MPMS XL SQUID susceptometer in the temperature range of 2–300 K.

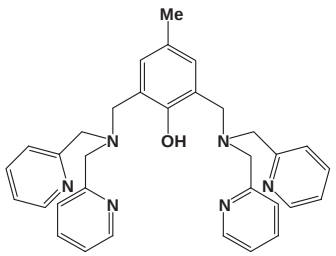

Fig. 1. Chemical structure of Hbpmp.

Preparation. Hbpmp was prepared by the literature method.[23] Other chemicals were purchased from commercial sources and used without further purification. $[M_2(dpmp)(bnp)_2]ClO_4$ (M = Mn (**1**), Ni (**2**), and Zn (**3**)) were prepared by two methods given below.

Method I. A solution of $M(ClO_4)_2 \cdot 6H_2O$ (M = Mn, Ni, or Zn) (1.0 mmol) in hot methanol (5 mL) was added to a solution of Hbpmp (0.5 mmol) in hot methanol (10 mL), and the mixture was stirred at ambient temperature for 30 minutes. A solution of sodium bis(*p*-nitrophenyl) phosphate (NaBNP) (1.0 mmol) in methanol (5 mL) was added, and the mixture was stirred for 30 minutes and allowed to stand to give $[M_2(dpmp)(bnp)_2]ClO_4$ as microcrystals.

Method II. A methanol solution of the bis(μ-acetato) complex of $bpmp^-$, $[M_2(bpmp)(AcO)_2]ClO_4$ (M = Mn,[24] Ni,[25] Zn[26]), and NaBNP in the 1:2 molar ratio was refluxed for one hour and the

† Present address: Graduate School of Engineering, Department of Synthetic Chemistry and Biological Chemistry, Kyoto University, Katsura, Nishikyo-ku, Kyoto 615-8510

Published on the web June 6, 2005; DOI 10.1246/bcsj.78.1072

mixture was concentrated to obtain $[M_2(dpmp)(bnp)_2]ClO_4$.

$[Mn_2(bpmp)(bnp)_2]ClO_4$ (1). Colorless microcrystals. Yield by method I: 72%. Calcd for $C_{57}H_{49}ClMn_2N_{10}O_{21}P_2$: C, 48.30; H, 3.48; N, 9.88; Mn, 7.75%. Found: C, 48.23; H, 3.50; N, 9.92; Mn 7.80%. Selected IR data [ν/cm^{-1}] using KBr: 1605, 1592, 1520, 1490, 1348, 1267, 1219, 1114, 1096, 913, 768, 623, 555. UV–vis data [λ/nm (ε/M^{-1} cm^{-1})] in DMSO: 280 (37000), 308 (39000).

$[Ni_2(bpmp)(bnp)_2]ClO_4$ (2). Blue microcrystals. Yield by method I: 81%. Calcd for $C_{57}H_{49}ClN_{10}O_{21}P_2Ni_2$: C, 48.05; H, 3.47; N, 9.83; Ni, 8.24%. Found: C, 47.98; H, 3.37; N, 9.84; Ni 8.30%. Selected IR data [ν/cm^{-1}] using KBr: 1609, 1592, 1520, 1348, 1271, 1220, 1097, 905, 767, 623, 551. UV–vis data [λ/nm (ε/M^{-1} cm^{-1})] in DMSO: 280 (39000), 305 (41000), 597 (14), 988 (37).

$[Zn_2(bpmp)(bnp)_2]ClO_4$ (3). Colorless microcrystals. Yield by method I: 45%. Calcd for $C_{57}H_{49}ClN_{10}O_{21}P_2Zn_2$: C, 47.60; H, 3.43; N, 9.74; Zn, 9.09%. Found: C, 47.48; H, 3.44; N, 9.72; Zn, 8.61%. Selected IR data [ν/cm^{-1}] using KBr: 1608, 1592, 1520, 1348, 1270, 1219, 1095, 910, 623, 553. UV–vis data [λ/nm (ε/M^{-1} cm^{-1})] in DMSO: 280 (38000), 305 (40000).

X-ray Crystallography. Single crystals of **1**·2MeCN were grown by slow recrystallization of **1** from acetonitrile. A single crystal was mounted on a glass fiber and coated by epoxy resin. Crystallographic measurements were made on a Rigaku/MSC Mercury diffractometer at −95 °C with graphite monochromated Mo Kα radiation (λ = 0.71070 Å). A symmetry-related absorption correction using the program ABSCOR and an empirical absorption correction based on azimuthal scans of several reflections were applied. Pertinent crystallographic parameters are summarized in Table 1.

The structure was solved by the direct method and expanded using the Fourier technique. Non-hydrogen atoms were refined anisotropically. Hydrogen atoms were included in the structure analysis but not refined. All calculations were performed using the teXsan crystallographic software package of Molecular Structure Corporation.[27]

Crystallographic data have been deposited at the CCDC, 12 Union Road, Cambridge CB2 1EZ, UK and copies can be obtained on request, free of charge, by quoting the publication citation and deposition number CCDC 256446.

Table 1. Crystallographic Data of $[Mn_2(bpmp)(bnp)_2]$-ClO_4·2MeCN (**1**·2MeCN)

Formula	$C_{61}H_{55}ClMn_2N_{12}O_{21}P_2$
Formula weight	1499.44
Crystal system	orthorhombic
Space group	$P\bar{1}$
a/Å	12.3628(4)
b/Å	13.2771(4)
c/Å	20.5465(7)
α/degree	83.208(7)
β/degree	85.361(7)
γ/degree	76.624(5)
V/Å^3	3253.03(18)
Z value	2
D_{calc}/g cm^{-3}	1.531
μ(Mo Kα)/cm^{-1}	5.65
No. reflections	13996
R	0.096
R_w	0.232

Results and Discussion

Crystal Structures. An ORTEP[28] view of **1**·2MeCN is shown in Fig. 2 together with selected atom numberings. Relevant bond distances and angles are summarized in Table 2.

The asymmetric unit consists of one $[Mn_2(bpmp)(bnp)_2]^+$ cation, one perchlorate ion and two acetonitrile molecules. The perchlorate ion and the acetonitrile molecules are free

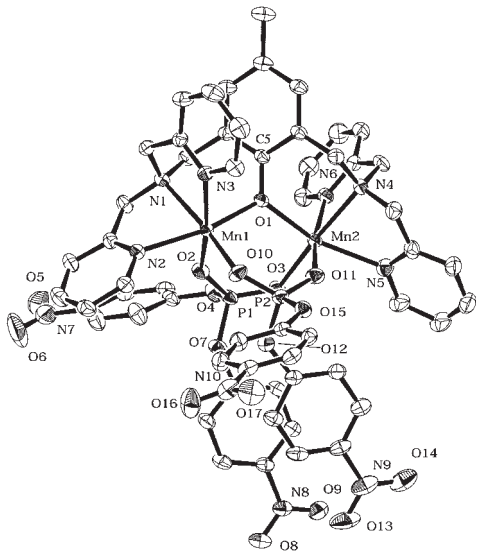

Fig. 2. An ORTEP view of $[Mn_2(bpmp)(bnp)_2]ClO_4$·2MeCN (**1**·2MeCN).

Table 2. Selected Bond Distances and Angles of **1**·2MeCN

Bond distances (Å)			
Mn(1)–O(1)	2.112(2)	Mn(1)–O(2)	2.168(3)
Mn(1)–O(10)	2.101(3)	Mn(1)–N(1)	2.280(3)
Mn(1)–N(2)	2.258(3)	Mn(1)–N(3)	2.241(3)
Mn(2)–O(1)	2.126(2)	Mn(2)–O(3)	2.134(3)
Mn(2)–O(11)	2.206(3)	Mn(2)–N(4)	2.298(3)
Mn(2)–N(5)	2.298(3)	Mn(2)–N(6)	2.249(3)
Mn(1)···Mn(2)	3.68		
Bond angles (degree)			
O(1)–Mn(1)–O(2)	86.6(1)	O(1)–Mn(1)–O(10)	101.6(1)
O(1)–Mn(1)–N(1)	88.8(1)	O(1)–Mn(1)–N(2)	159.0(1)
O(1)–Mn(1)–N(3)	89.3(1)	O(2)–Mn(1)–O(10)	100.1(1)
O(2)–Mn(1)–N(1)	88.6(1)	O(2)–Mn(1)–N(2)	82.4(2)
O(2)–Mn(1)–N(3)	165.0(2)	O(10)–Mn(1)–N(1)	166.7(1)
O(10)–Mn(1)–N(2)	97.9(2)	O(10)–Mn(1)–N(3)	94.9(1)
N(1)–Mn(1)–N(2)	73.2(1)	N(1)–Mn(1)–N(3)	76.8(1)
N(2)–Mn(1)–N(3)	96.7(1)	O(1)–Mn(2)–O(3)	98.4(1)
O(1)–Mn(2)–O(11)	91.0(1)	O(1)–Mn(2)–N(4)	87.2(1)
O(1)–Mn(2)–N(5)	157.9(1)	O(1)–Mn(2)–N(6)	91.1(1)
O(3)–Mn(2)–O(11)	94.2(2)	O(3)–Mn(2)–N(4)	171.4(1)
O(3)–Mn(2)–N(5)	102.8(1)	O(3)–Mn(2)–N(6)	97.1(2)
O(11)–Mn(2)–N(4)	92.3(1)	O(11)–Mn(2)–N(5)	81.2(1)
O(11)–Mn(2)–N(6)	168.1(1)	N(4)–Mn(2)–N(5)	72.6(1)
N(4)–Mn(2)–N(6)	76.2(1)	N(5)–Mn(2)–N(6)	92.6(2)
Mn(1)–O(1)–Mn(2)	119.9(1)		

from coordination and captured in the crystal lattice. Two Mn ions in $[Mn_2(bpmp)(bnp)_2]^+$ are bridged by the phenolic oxygen atom of $bpmp^-$ and by two BNP^- groups. The Mn(1)···Mn(2) interatomic separation is 3.68 Å and the Mn(1)–O(1)–Mn(2) angle is 119.9(1)°. Each Mn has a six-coordinate geometry with an average Mn-to-donor bond distance of 2.195 Å for Mn(1) and 2.218 Å for Mn(2). Two pyridine residues on each articular nitrogen atom (N(1) and N(4)) are not equivalent in the crystal: one pyridine nitrogen (N(2) or N(5)) is situated trans to the phenolic oxygen O(1), whereas the other pyridine nitrogen (N(3) or N(6)) is situated cis to O(1). When the plane defined by O(1), N(1), and N(2) (O(1), N(4), and N(5)) is assumed to be the equatorial base, each BNP^- ion makes a bond to an equatorial site of one Mn and to an apical site of another Mn. As the result, the complex molecule shows a twist with respect to the C(5)–O(1) bond of the phenol group. The twist angle between the phenolic ring and the least-squares plane defined by Mn(1), O(1), and Mn(2) is 51.3(1)°. The P(1)–O(2), P(1)–O(3), P(2)–O(10), and P(2)–O(11) bond lengths fall in the range of 1.473(3)–1.488(3) Å.

It is of value to compare the structure of **1**·2MeCN with the structure of the analogous bis(μ-acetato) complex, $[Mn_2(bpmp)(AcO)_2]ClO_4$.[29] This complex has the Mn(1)···Mn(2) separation of 3.412 Å and the Mn(1)–O(1)–Mn(2) angle of 107.9°. Thus, the Mn···Mn separation and the Mn(1)–O(1)–Mn(2) angle in **1**·2MeCN are enlarged relative to those of $[Mn_2(bpmp)(AcO)_2]ClO_4$.

The bis(μ-acetato) dinickel(II) complex, $[Ni_2(bpmp)(AcO)_2]BF_4$,[26] has the Ni(1)···Ni(2) separation of 3.40 Å and the Ni(1)–O(1)–Ni(2) angle of 114.5°. The twist angle between the phenolic ring and the least-squares plane defined by Ni(1), O(1), and Ni(2) is 47.3°. A similar twist angle is recognized for $[Zn_2(bpmp)(AcO)_2]BF_4$·2MeOH (48.8°).[25]

Properties. The IR spectral assignments of **1**–**3** are made by comparison with the IR spectra of $[M_2(bpmp)(AcO)_2](ClO_4)_2$ (M = Mn, Ni, Zn).[24–26] Two intense bands at 1520 and 1348 cm^{-1} are assigned to the $\nu_{as}(NO_2)$ and $\nu_s(NO_2)$ vibrations of the nitro group of BNP^-, respectively. Two prominent bands at 1270–1271 and 1219–1220 cm^{-1} are attributed to ν(P=O) vibrations of the bridging BNP^- group.

Each electronic absorption spectrum of **1**–**3** in DMSO has two intense bands at 280 and 305–308 nm. The band at 280 nm is assigned to an intra-ligand transition associated with $bpmp^-$ and the band at 305–308 nm to an intra-ligand band associated with BNP^- ion. Complex **2** shows two weak bands at 597 and 988 nm which can be assigned to the $^3T_{1g}(F) \leftarrow {}^3A_{2g}(F)$ and $^3T_{2g}(F) \leftarrow {}^3A_{2g}(F)$ transitions, respectively, of octahedral Ni(II).[30] The spectra of **1**–**3** were practically independent of concentration for 10^{-4}–10^{-6} M^{-1}, indicating the considerable stability of the $[M_2(bpmp)(AcO)_2]^+$ core in DMSO solution.

The magnetic moment of **1** at room temperature is 5.70 μ_B per Mn and the moment decreased with decreasing temperature to 0.52 μ_B at 2 K (Fig. 3). This fact means an antiferromagnetic interaction between the two Mn(II) ions. Magnetic analyses were carried out using the magnetic susceptibility expression for ($S_1 = 5/2$)–($S_2 = 5/2$) based on the isotropic Heisenberg model ($\boldsymbol{H} = -2J\boldsymbol{S}_1\boldsymbol{S}_2$):[31]

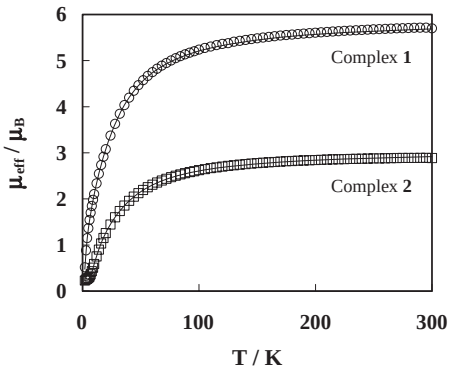

Fig. 3. Temperature-dependence of magnetic moment of $[Mn_2(bpmp)(bnp)_2]ClO_4$ (**1**) (top) and $[Ni_2(bpmp)(bnp)_2]ClO_4$ (**2**) (bottom).

$$\chi_A = \{Ng^2\beta^2/kT\} \times [\exp(-28J/kT) + 5\exp(-24J/kT) + 14\exp(-18J/kT) + 30\exp(-10J/kT) + 55]/[\exp(-30J/kT) + 3\exp(-28J/kT) + 5\exp(-24J/kT) + 7\exp(-18J/kT) + 9\exp(-10J/kT) + 11]. \quad (1)$$

In this equation N is Avogadro's number, g is the Lande g factor, β is the Bohr magneton, k is the Boltzmann constant, T is the absolute temperature, and J is the exchange integral. As shown by the solid lines in Fig. 3, a good magnetic simulation is obtained using the best-fit parameters of $J = -2.72$ cm^{-1} and $g = 2.00$.

The magnetic moment of **2** at room temperature is 2.88 μ_B (per Ni) and the moment decreases with decreasing temperature to 0.23 μ_B at 2 K (Fig. 3). The χ_A vs T curve shows a slight increase below 6 K, implying some contamination of a small amount of a paramagnetic impurity. Magnetic analyses were carried out using the magnetic susceptibility expression for ($S_1 = 1$)–($S_2 = 1$) based on the isotropic Heisenberg model and taking into consideration a fraction (ρ) of paramagnetic impurity:

$$\chi_A = (1-\rho)\{Ng^2\beta^2/kT\} \times [5 + \exp(-4J/kT)]/[5 + 3\exp(-4J/kT) + \exp(-6J/kT)] + \rho \times (g^2/4T) + N\alpha. \quad (2)$$

In this equation, $N\alpha$ is the temperature-independent paramagnetism and other symbols have the same physical meanings as in Eq. (1). The cryomagnetic behavior of **2** is well reproduced using the best-fit parameters of $J = -13.3$ cm^{-1}, $g = 2.14$, $N\alpha = 120 \times 10^{-6}$ $cm^3\,mol^{-1}$ and $\rho = 0.006$. Complex **1** shows a slightly weak antiferromagnetic interaction relative to $[Mn_2(bpmp)(AcO)_2]ClO_4$ ($J = -4.8$ cm^{-1})[24,29] whereas **2** shows a strong antiferromagnetic interaction relative to $[Ni_2(bpmp)(AcO)_2]BF_4$ ($J = -2.3$ cm^{-1}).[26]

The magnetic interaction in bis(μ-acetato)-μ-phenolato dinuclear complexes is essentially mediated by the phenolic oxygen atom.[32,33] This must be also the case of bis(μ-bnp)-μ-phenolato dinuclear complexes. The exchange integral of dinuclear Ni^1(II)–Ni^2(II) (d^8–d^8) is given by the mean of four one-electron exchange integrals,

$$J = (1/4)[j(d_{x^2-y^2}, d_{x^2-y^2}) + j(d_{x^2-y^2}, d_{z^2}) + j(d_{z^2}, d_{x^2-y^2}) + j(d_{z^2}, d_{z^2})], \quad (3)$$

where local x and y axes are taken on each metal. In general, $j(d_{x^2-y^2}, d_{x^2-y^2})$ is dominant among the four one-electron exchange integrals,[34] so the magneto-structural correlation established for Cu(II)–Cu(II) (d^9–d^9)[35–37] can be applied to dinuclear nickel(II) complexes. The $j(d_{x^2-y^2}, d_{x^2-y^2})$ integral of μ-hydroxo- and μ-phenolato dinuclear complexes depends upon the M–O–M angle and a stronger antiferromagnetic interaction occurs when the M–O–M angle becomes larger. As inferred from the comparison of the Mn–O–Mn angle of **1**·2MeCN (119.9°) and the Mn–O–Mn angle of $[Mn_2(bpmp)(AcO)_2]ClO_4$ (107.9°), $[Ni_2(bpmp)(bnp)_2]ClO_4$ (**2**) must have a large Ni–O–Ni angle relative to that of $[Ni_2(bpmp)(AcO)_2]BF_4$ (114.5°). The enhanced antiferromagnetic interaction of **2** can be explained by the enlargement of the Ni–O–Ni angle (Fig. 4) that gives rise to an efficient spin exchange through the $d_{x^2-y^2}(Ni^1)||p_\sigma(O)||d_{x^2-y^2}(Ni^2)$ pathway.

The exchange integral of dinuclear Mn^1(II)–Mn^2(II) (d^5–d^5) is given by the mean of 25 one-electron exchange integrals, $j(d_k, d_l)$,

$$J = (1/25)\Sigma j(d_k, d_l), \quad (4)$$

where d_k and d_l represent one of the five d-orbitals ($d_{x^2-y^2}$, d_{z^2}, d_{xy}, d_{xz}, and d_{yz}) of Mn^1 and Mn^2, respectively. The sign and the magnitude of each $j(d_k, d_l)$ depend complicatedly upon structure, and because of this reason no magneto-structural correlation has been established for dinuclear manganese(II) complexes. In general, the J value for dinuclear manganese(II) complexes is small ($-J < 5$ cm^{-1}) as the result of the compensation of positive and negative $j(d_k, d_l)$ components.

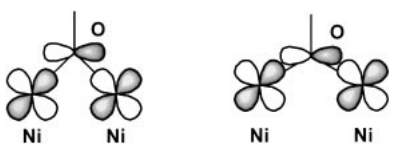

Fig. 4. Schematic illustration of antiferromagnetic interaction in μ-phenolato dinickel(II) through $d_{x^2-y^2}$(Ni)-$\|p_\sigma$(O)$\|d_{x^2-y^2}$(Ni) pathway: (left) for a small Ni–O–Ni angle and (right) for a large Ni–O–Ni angle.

Relevance to Biological Phosphodiesterase. The compartmental ligands of the "end-off" type, 2,6-bis{*N*-[2-(dimethylamino)ethyl]iminomethyl}-4-methylphenol (HL^1), 2-{*N*-[2-(dimethylamino)ethyl]iminomethyl}-6-{*N*-methyl-*N*-[2-(dimethylamino)ethyl]aminomethyl}-4-bromophenol (HL^2), and 2,6-bis{2-[(2-pyridyl)ethyl]iminomethyl}-4-methylphenol (HL^3) (Fig. 5), are often used along with Hbpmp for modeling bimetallic biosites. We have found that the dinuclear manganese(II) complexes of HL^1–HL^3 hydrolyze BNP^-, whereas the dinuclear nickel(II) and zinc(II) complexes of HL^1–HL^3 have little activity to hydrolyze BNP^-.[38] The dinuclear manganese(II) complexes of L^1–L^3 illustrate the significance of a pair of Mn ions in biological hydrolysis of a phosphodiester and can be regarded as functional models of Mn phosphodiesterases.[10] Based on preliminary mass spectrometric studies, a μ-acetato-μ-bnp species, $[M_2(L^1)(AcO)(bnp)]^+$ (M = Mn, Ni, Zn), is produced in solution (along with a small amount of bis-μ-bnp species, $[M_2(L^1)(bnp)_2]^+$) when $[M_2(L^1)(AcO)_2]ClO_4$ is treated with one equivalent of HBNP in DMSO.[38] Obviously the bridging acetate group is readily replaced with BNP^-, in harmony with the derivation of **1**–**3** from $[M_2(bpmp)(AcO)_2]ClO_4$ in this work. We have also confirmed that the mass peak of $[Mn_2(L^1)(AcO)(bnp)]^+$ diminishes with time and finally disappears, but the mass peak of $[Ni_2(L^1)(AcO)(bnp)]^+$ and the mass peak of $[Zn_2(L^1)(AcO)(bnp)]^+$ remain intact. We presume that the hydrolysis of BNP^- by the dinuclear manganese(II) complexes of HL^1–HL^3 occurs through the $[Mn_2(L)(AcO)(bnp)]^+$ (and $[Mn_2(L)(bnp)_2]^+$) intermediate.

In this regard, we are interested in the behavior of **1** in hydrous solvents, and we found that the bound BNP^- in **1**, as well as the bound BNP^- in **2** and **3**, is not hydrolyzed in hydrous DMSO, in marked contrast to the case of $[Mn_2(L^1)(AcO)(bnp)]^+$. The substantial difference between **1** and $[Mn_2(L^1)(AcO)(bnp)]^+$ is in the coordination number about the metal center. In the case of $[Mn_2(L^1)(AcO)(bnp)]^+$, the Mn center has a five-coordinate geometry, so that it can accommodate a water molecule for hydrolyzing the bound BNP^-.[38] In the case of **1**, the Mn center in a six-coordinate environment cannot accommodate a water molecule for hydrolyzing the bound BNP^-. This must also be the case of analogous $[FeZn(bpmp)(dpp)_2]ClO_4$ with diphenyl phosphate (DPP^-);[20] the bridging DPP^- seems to be inert to hydrolysis.

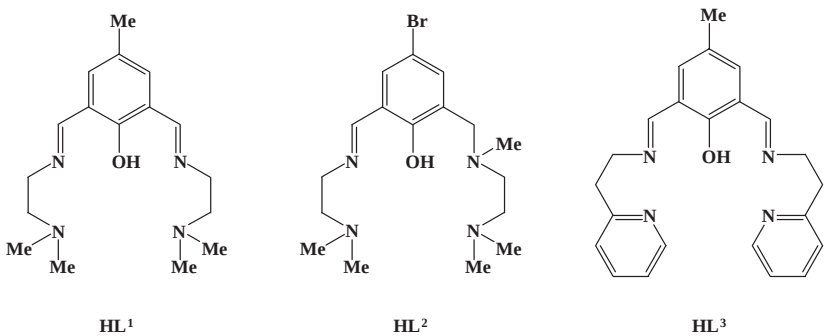

Fig. 5. Chemical structures of 2,6-bis{*N*-[2-(dimethylamino)ethyl]iminomethyl}-4-methylphenol (HL^1), 2-{*N*-[2-(dimethylamino)ethyl]iminomethyl}-6-{*N*-methyl-*N*-[2-(dimethylamino)ethyl]aminomethyl}-4-bromophenol (HL^2), and 2,6-bis{2-[(2-pyridyl)ethyl]iminomethyl}-4-methylphenol (HL^3).

Conclusion

2,6-Bis[*N*,*N*-di(2-pyridylmethyl)aminomethyl]-4-methylphenol (Hbpmp) forms dinuclear Mn(II), Ni(II), and Zn(II) complexes with two bis(*p*-nitrophenyl) phosphate (BNP^-) ions: $[M_2(bpmp)(bnp)_2]ClO_4$ (M = Mn (**1**), Ni (**2**), and Zn (**3**)). Complexes **1**–**3** are also derived from the bis(acetato) complexes, $[M_2(bpmp)(AcO)_2]ClO_4$, by the treatment with NaBNP. The crystal structure of **1** is determined to have a bis(μ-bnp)-μ-phenolato dinuclear core. Complex **1** exhibits a weak antiferromagnetic interaction ($J = -2.72$ cm^{-1}) and complex **2** exhibits a moderate antiferromagnetic interaction ($J = -13.3$ cm^{-1}). The enhanced antiferromagnetic interaction in **2** relative to $[Ni_2(bpmp)(AcO)_2]BF_4$ ($J = -2.3$ cm^{-1}) is explained by a large Ni–O–Ni angle that allows an efficient spin exchange through the $d_{x^2-y^2}$(Ni)||p_σ(O)||-$d_{x^2-y^2}$(Ni) pathway. The bound BNP^- of the complexes is not hydrolyzed in hydrous DMSO, because the metal center in a six-coordinate environment cannot accommodate a water molecule for hydrolysis.

This work was supported by a Grant-in-Aid for Scientific Research (No. 07454178) from the Ministry of Education and Technology.

References

1 D. E. Fenton and H. Ōkawa, "Perspectives on Bioinorganic Chemistry," JAI Press, London (1993), Vol. 2, p 81.

2 J. L. Vanhooke, M. M. Benning, F. M. Raushel, and H. M. Holden, *Biochemistry*, **35**, 6020 (1996).

3 E. Hough, L. K. Hansen, B. Birkness, K. Jynge, S. Hansen, A. Hardvik, C. Little, E. J. Dodson, and Z. Derewenda, *Nature*, **338**, 357 (1989).

4 A. Lahm, S. Volbeda, F. Sakijama, and D. Suck, *J. Mol. Biol.*, **215**, 207 (1990).

5 E. E. Kim and H. W. Wyckoff, *J. Mol. Biol.*, **218**, 449 (1991).

6 L. Que, Jr. and A. E. True, *Prog. Inorg. Chem.*, **38**, 91 (1990).

7 a) S. K. Burley, R. R. David, R. M. Sweet, A. Taylor, and W. N. Lipscomb, *J. Mol. Biol.*, **224**, 113 (1992). b) C. R. Kissinger, H. E. Parge, D. R. Knighton, C. T. Lewis, L. A. Pelletier, A. Tempczyk, V. J. Kalish, K. D. Tucker, R. E. Showalter, E. W. Moomaw, L. N. Gastinel, N. Habuka, X. Chen, F. Maldonado, J. E. Barker, R. Bacquet, and E. Villafranca, *Nature*, **378**, 641 (1995).

8 M. P. Engloff, P. T. W. Cohen, P. Reinemer, and D. Barford, *J. Mol. Biol.*, **254**, 942 (1995).

9 J. Goldberg, H. Huang, Y. Kwon, P. Greengard, A. C. Nairn, and J. Kuriyan, *Nature*, **376**, 745 (1995).

10 A. K. Das, N. R. Helps, P. T. W. Cohen, and D. Barford, *EMBO J.*, **15**, 6798 (1996).

11 E. Bernard, S. Chardon-Noblat, A. Deronzier, and J.-M. Latour, *Inorg. Chem.*, **38**, 190 (1999).

12 F. Verge, C. Lebrum, M. Fontecave, and S. Ménage, *Inorg. Chem.*, **42**, 499 (2003).

13 D. H. Vance and A. W. Czarnik, *J. Am. Chem. Soc.*, **115**, 12165 (1993).

14 M. J. Yound and J. Chin, *J. Am. Chem. Soc.*, **117**, 10577 (1995).

15 H. Machinaga, K. Matsufuji, M. Ohba, M. Kodera, and H. Ōkawa, *Chem. Lett.*, **2002**, 716.

16 M. Lanznaster, A. Neves, A. J. Bortoluzzi, B. Szpoganicz, and E. Schwingel, *Inorg. Chem.*, **41**, 5641 (2002).

17 M. Yamami, H. Furutachi, T. Yokoyama, and H. Ōkawa, *Inorg. Chem.*, **37**, 6832 (1998).

18 K. Arimura, M. Ohba, T. Yokoyama, and H. Ōkawa, *Chem. Lett.*, **2001**, 1134.

19 C. Bazzicalupi, A. Bencini, A. Bianchi, V. Fusi, C. Giorgi, P. Paoletti, B. Valtancoli, and D. Zanchi, *Inorg. Chem.*, **36**, 2784 (1997).

20 K. Schepers, B. Bremer, B. Krebs, G. Henkel, E. Althaus, B. Mosel, and W. Müller-Warmuth, *Angew. Chem., Int. Ed. Engl.*, **29**, 531 (1990).

21 T. Tanase, J. W. Yun, and S. J. Jippard, *Inorg. Chem.*, **35**, 3585 (1996).

22 C. He and S. J. Lippard, *J. Am. Chem. Soc.*, **122**, 184 (2000).

23 M. Suzuki, H. Kanatomi, Y. Demura, and I. Murase, *Bull. Chem. Soc. Jpn.*, **57**, 1003 (1984).

24 M. Suzuki, M. Mikuriya, S. Murata, A. Uehara, H. Oshio, S. Kida, and K. Saito, *Bull. Chem. Soc. Jpn.*, **60**, 4305 (1987).

25 L. Que, Jr., T. R. Holman, and M. P. Hendrich, *Inorg. Chem.*, **31**, 939 (1992).

26 H. Adams, D. Bradshaw, and D. E. Fenton, *Inorg. Chim. Acta*, **332**, 195 (2002).

27 teXsan Crystal Structure Analysis Package, Molecular Structure Corporation, Houston, TX (1985 and 1999).

28 C. K. Johnson, Report 3794, Oak Ridge National Laboratory, Oak Ridge, TN (1965).

29 S. Blanchard, G. Blondin, E. Riviere, M. Nierlich, and J. Girerd, *Inorg. Chem.*, **42**, 4658 (2003).

30 D. B. Powell and N. Sheppard, *Spectrochim. Acta*, **17**, 68 (1961).

31 a) J. H. van Vleck, "The Theory of Electric and Magnetic Susceptibilities," Oxford University Press, London (1932). b) P. A. M. Dirac, "The Principle of Quantum Mechanics," Oxford University Press, London (1958).

32 W. H. Armstrong and S. J. Stephen, *J. Am. Chem. Soc.*, **106**, 4632 (1984).

33 R. Hotzelmann, K. Wieghardt, J. Ensling, H. Romstedt, P. Gütlich, E. Bill, U. Flörke, and H.-J. Haupt, *J. Am. Chem. Soc.*, **114**, 9470 (1992).

34 C. J. Cairns and D. H. Busch, *Coord. Chem. Rev.*, **69**, 1 (1986).

35 D. L. Lewis, K. T. McGregor, W. E. Hatfield, and D. J. Hodgson, *Inorg. Chem.*, **13**, 1013 (1973).

36 P. J. Hay, J. C. Thibeault, and R. Hoffmann, *J. Am. Chem. Soc.*, **97**, 4884 (1975).

37 M. Handa, N. Koga, and S. Kida, *Bull. Chem. Soc. Jpn.*, **61**, 3853 (1988).

38 R. Jikido, Master Thesis, Faculty of Science, Kyushu University (2004). Manuscript has been prepared for publication.